Supporting Information

Electrolytic Upcycling of PET Waste Plastics for Energy-Efficient Hydrogen Evolution

Guohao Xu,[a] Zhaopeng Sun,[a] Kai He,[a] Wei Liu,*[a] Xinyue He,[a] Kai Liu,[a] Binjie Zhou,[b] Jichang Liu,[c] and Yulin Deng[d]

[a]School of Chemistry and Chemical Engineering, Central South University, Changsha, 410083, China.

E-mail: wliu300@csu.edu.cn (Wei Liu)

[b]National Engineering Laboratory for Mobile Source Emission Control Technology, China Automotive Technology & Research Center Co., Ltd., Tianjin, 300300, China

[c]State Key Laboratory of Chemical Engineering, East China University of Science and Technology, Shanghai, 200237, China

[d]School of Chemical & Biomolecular Engineering and RBI at Georgia Tech, Georgia Institute of Technology, 500 10th Street N.W., Atlanta, GA 30332-0620, USA

Experimental Section

Materials

PET powder (2000 mesh) was purchased from Shanghai Ruitao Import and Export Co., LTD. Phosphomolybdic acid ($H_3[PMo_{12}O_{40}]$, noted as PMo_{12}) was purchased from TCI America. Terephthalic acid (noted as TPA), Graphite felt, Sodium hydroxide (NaOH) and Perchloric acid (70%, $HClO_4$) were purchased from Alfa Aesar. Phosphoric acid (85%, H_3PO_4), Deuterium oxide (D_2O, 99.9 %), Glycol terephthalate, Dimethyl sulfoxide-d6 (DMSO-d6, 99.9%) and Trifluoromethanesulfonic acid (99%, noted as HTOf) was purchased from Macklin. Sulfuric acid (98%, H_2SO_4), Hydrochloric acid (37%, HCl) and Nitric acid (68%, HNO_3) were purchased from Sinopharm Chemical Reagent. High-purity water with a resistivity of 18.2 MΩ•cm was used for all the experimental procedures.

General procedures for PET hydrolysis

For the PET hydrolysis experiments, 1.0 g of PET powder (2000 mesh) and PMo_{12}-acid solution (0.1 mol L^{-1} PMo_{12}, 0.8 mol L^{-1} H_3PO_4, 10 mL) were added into a glass vial with a screw cap under continuous heating at 100 °C with a magnetic stirring (phosphoric acid was added into PMo_{12}-acid reaction system to prevent precipitation of PMo_{12} and allow easy TPA separation.). In order to prevent the effects of oxygen, air in the vessel was purged by pure N_2 gas before heating. When the reaction was completed, the reaction mixture was poured into about 40-60 mL of distilled water for terephthalic acid (TPA) precipitation and separation. To calculate the PET conversion and TPA yield, the precipitates were re-solubilized with an aqueous solution of NaOH (1 mol L^{-1}). The unreacted PET (if any) which is insoluble in an alkaline medium was removed by filtration and the produced TPA was recrystallized by hydrochloric acid. PET conversion was calculated using the following equation (1):

$$\text{PET conversion (\%)} = \frac{W_1 - W_2}{W_1} \times 100\ (\%) \qquad \text{Equation (1)}$$

where W_1 is the initial weight of PET powder and W_2 is the weight of unreacted PET.

TPA was finally precipitated by adding a certain amount of hydrochloric acid (1 mol L^{-1}) and then collected by filtration. The obtained white powder of TPA was then washed with water several times and dried at 80 °C overnight. TPA yield was calculated using the following equation (2):

$$\text{TPA yield (\%)} = \frac{W_3 M_{PET}}{M_{TPA} W_1} \times 100\ (\%) \qquad \text{Equation (2)}$$

where W_3 is the weight of Produced TPA, M_{TPA} is the molecular weight of TPA and M_{PET} is the molecular weight of the PET monomeric unit.

In order to analyze the kinetic character of the PET hydrolysis reaction, the first-order kinetic equation was used to fit the experiment data:

$$\ln\frac{1}{1-X}=kt \qquad \text{Equation (3)}$$

where X, k, and t are the PET conversion, the reaction rate constant, and the reaction time, respectively.

The Arrhenius equation was used to calculate the active energy of PET hydrolysis reaction under different conditions:

$$\ln k=\ln A-\frac{E_a}{RT} \qquad \text{Equation (4)}$$

where k is the reaction rate constant, A is the preexponential factor, R is the gas constant (8.314 J k^{-1} mol^{-1}), and T is the absolute temperature in Kelvin.

Assembly of electrolysis cell and test methods

The electrolytic cell consisted of bipolar plates, a proton exchange membrane and end plates. The bipolar plates of the electrolysis cell were made of high-density graphite plates with a serpentine flow channel 2 mm wide, and 10 mm deep (total geometry projected area of 1 cm^2 or 20 cm^2). The graphite felt was pretreated with concentrated H_2SO_4 and HNO_3 in a 3:1 volumetric ratio at 50 °C for 30 min. Then the graphite felt was washed with deionized water until the pH of the wash became neutral, dried at 80 °C and cut to pieces with 2 mm width and 10 mm thick. These graphite electrodes were filled into the channel of the anode plant. The anode electrode was graphite felt and the cathode of the cell was a commercial Pt/C modified electrode. The loading of Pt was about 4 mg/cm^2, which was calculated through the weight change of the cathode electrode before and after modification. Nafion 117® was used as a proton exchange membrane sandwiched between two graphite plates, which was pretreated firstly in the boiling solution of 1 mol L^{-1} H_2SO_4 and 3% H_2O_2 for 60 min, then washed with deionized water.

In the electrolysis experiments, the reduced PMo_{12} solution and H_3PO_4 solution (1 mol L^{-1}) were pumped through the anode and cathode cell, respectively, at a flow of 100 mL min^{-1}. An electrochemical working station (Gamry INTERFACE1010E) was used to record the polarization curves of the solution at different voltages. The hydrogen volume at the cathode was collected by drainage method. The linear cyclic voltammetry curves were measured using an Ag/AgCl reference electrode, a Pt wire counter electrode and a graphite working electrode with the scan rate 50 mV s^{-1} at 25 °C.

Recycling experiments of PET conversion and hydrogen evolution

As described in the PET hydrolysis experiments, 1.0 g of PET powder (2000 mesh) and PMo_{12}-acid solution (0.1 mol L^{-1} PMo_{12}, 2.5 mol L^{-1} H_2SO_4 or HTOf and 0.8 mol L^{-1} H_3PO_4,10 mL) were added into the reactor and heated 10 hours at 100 ^{o}C. The solution changed the color from yellow to dark blue. At the end of the hydrolysis reaction, the solid was separated by filtration, the liquid was used for electrolytic regeneration. In the electrolysis experiments, the reduced PMo_{12} solution and H_3PO_4 solution (1 mol L^{-1}) were pumped through the anode and cathode cell (with electrode area 20 cm^2) respectively, at a flow of 100 mL min^{-1}. An electrochemical working station (Gamry INTERFACE1010E) was used to record the polarization curves of the solution at different voltages. The hydrogen volume at the cathode was collected by drainage method. After the electrolysis, the color of the solution was changed from blue to initial yellow, and 1.0 g of PET powder could be newly added into the solution for next recycle of PET conversion.

Other characterizations

The XRD measurements were performed using a diffractometer (Rigaku Ultima IV) in a 2θ range of 10-50° with a scanning rate of 10° min^{-1}. The ^{1}H NMR analysis of ethylene glycol (EG) and ^{31}P NMR analysis (H_3PO_4 was used as the external reference) of 0.1 mol L^{-1} PMo_{12} and the mixture of 0.1 mol L^{-1} PMo_{12} and 2.5 mol L^{-1} HTOf (H_2SO_4 or $HClO_4$) in deuterium oxide were carried out with a NMR spectrometer (Bruker Avance III 500 MHz). The ^{1}H NMR analysis of TPA (5 g L^{-1}) in dimethyl sulfoxide-d6 was carried out with an NMR spectrometer (Bruker Avance III 500 MHz). The chemical structure characteristics of waste PET and the produced TPA were analyzed by FT-IR spectroscopy (SHIMADZU IR Spirit). UV-Vis absorption spectrum of reduced PMo_{12} was measured on the UV-Vis spectrophotometer (SHIMADZU UV-2600i Series). The Raman spectra were collected by a confocal Raman spectrometer (Renishaw, inVia Reflex) equipped with a diode laser emitting at 785 nm. GC (Agilent GC-8860) with both a hydrogen flame ionization detector (FID) and a thermal conductivity detector (TCD) was used to analyze the emissions of gas during the reaction process of PET hydrolysis.

Computational methods

All the Density functional theory (DFT) calculations were performed by using the Gaussian 16 package. The standard 6-31G(d) basis set was used for the main group elements; the pseudopotential basis set LANL2DZ was

selected for all metal atoms. The long-range van der Waals (vdW) interactions were accounted for using the DFT-D3 method. Frequency calculations were made to determine the characteristics of all stationary points as energy minima or transition states on the corresponding potential energy surfaces by the correct number of imaginary frequencies. The geometry optimization was full and without any symmetry constraints. The free energy correction was included in the free energy calculations using frequency calculations. Bulk solvent effects of water media were considered via the self-consistent reaction field method, using the integral equation formalism polarizable continuum model.

Life-cycle assessment

The LCA analysis followed the standard series ISO 14040 and was conducted using OpenLCA 2.0.3. The aim is to identify the optimal hydrolysis design to upgrade PET and to compare the results with virgin PET and other chemical recycling methods. The functional unit is 1000 g of produced TPA. The system boundary is cradle-to-gate, which includes: the collection and transportation of waste PET, the production of PET flakes and the whole process of depolymerization. Two environmental impact categories were assessed, namely global warming potential (GWP) and non-renewable energy use (NREU). Two geographical scopes were investigated, including China and Europe.

Table S1 Comparisons of PET acidic hydrolysis in this study with reported literatures.

NO.	Catalytic system	Acid concentration (mol L^{-1})	Temperature (^{o}C)	Time (h)	PET conversion or TPA yield (%)	Ref.
1	H_2SO_4	14	100	0.5	100	[1]
2	HNO_3	13	100	3.5	90	[2]
3	HNO_3	13	90	8	70	[2]
4	HNO_3	13	80	18	65	[2]
5	HNO_3	9.5	100	5	90	[2]
6	p-toluenesulfonic acid	23	150	1.5	100	[3]
7	Terephthalic acid	0.0012	220	3	100	[4]
8	DES: $FeCl_3$+ methanesulfonic acid	15.2	100	1	100	[5]
9	DES: $FeCl_3$+ methanesulfonic acid	15.2	100	3	100	[5]
10	Acetic acid	17.5	280	2	100	[6]
11	P-styrene sulfonic acid	2	150	14	60-70	[7]
12	H_2SO_4	7	150	5	100	[8]
13	HNO_3	13	100	16	90	[9]
14	0.25 M HTOf 0.5 M H_2O Acetic acid solvent	17.5	180	2	80-90	[10]
15	H_2SO_4 + H_3PO_4	12.5	140	2.7	97.8	[11]
16	PMo_{12}	0.5-1	100	4-10	90-100%	**This work**
17	PMo_{12}-HTOf	2.6	100	10	90.2%	**This work**

Table S2 The degradation of PET under alkaline conditions in the reported literatures.

NO.	Catalytic system	Alkaline concentration (mol L^{-1})	Temperature (°C)	Time (h)	PET conversion or TPA yield (%)	Ref.
1	NaOH and tributylhexadecylphosphoni-um bromide quaternary salt (TBHDPB) (TBHDPB : PET = 0.2)	1.75	100	4	≈93	12
2	NaOH and TBHDPB (TBHDPB : PET = 0.1)	1.75	100	4	87	12
3	NaOH and TBHDPB (TBHDPB : PET = 0.1)	1.75	90	4	≈78	12
4	NaOH and TBHDPB (TBHDPB : PET = 0.1)	1.75	80	4	≈65	12
5	NaOH and $[C_{16}H_{33}N(CH_3)_3]_3PW_{12}O_{40}$ (0.5%)	1.0	110	5	99	13
6	NaOH and $[C_{16}H_{33}N(CH_3)_3]_3PW_{12}O_{40}$ (0.5%)	2.0	110	3	≈98	13
7	NaOH and ethanol glycol (60%)	1.25	80	0.33	≈95	14
8	NaOH and ethanol glycol	0.75	110	6	78.4	15
9	NaOH and ethanol	0.75	80	2	91.8	15
10	NaOH and ethanol	0.5	80	2	88.6	15
11	KOH	2	60	16	96.7	16
12	KOH and long-chain alkyl quaternary ammonium functionalized hyperbranched polyester (QHPE)	0.2	98	1	≈25	17
13	NaOH and Hexadecyltrimethylammonium chloride	1.5	80	0.167	100	18
14	NaOH and tributylhexadecylphosphoni-um bromide (0.07 mol/L)	1.67	80	1	≈84	19
15	NaOH and tetraoctylphosphonium bromide (0.07 mol/L)	1.67	80	1	≈75	19
16	NaOH	1.125	200	1	97.9	20
17	NaOH	1.125	150	7	84.0	20
18	NaOH	1.125	120	7	33.0	20
19	NaOH and tetrabutyl ammonium iodide	2.5	90	1	100	21

Table S3 Summary of electrocatalytic PET conversion in the reported literatures.

NO.	Catalyst	Electrolyte	Potential (V)	Current density (mA cm^{-1})	Oxidative product	Faraday efficiency (%)	Ref.
1	Pt-$Ni(OH)_2$/NF	KOH	0.69 (vs RHE)	100	glycollic acid	93	[22]
2	$Ni(OH)_2$/NF	KOH	0.43 (vs RHE)	100	formate	93.2	[23]
3	$CoNi_{0.25}P$	KOH	1.8	500	formate	80	[16]
4	V_O-Co_3O_4/NF	KOH	1.31(vs RHE)	100	formate	91	[24]
5	Cobalt-vanadium layered double hydroxides	KOH	1.47	350	formate	91.33	[25]
6	CuO nanowire	KOH	0.26	10	formate	88	[26]
7	Pd-NiTe/NF	KOH	1.35	100	formate	95.6	[27]
8	Pd-CoNiP@NF	KOH	1.31	500	formate	90	[28]
9	CoFe-P/NF	KOH	1.52	20	formate	90	[29]
10	PtAg/NF	KOH	0.8	250	glycollic acid	95.2	[30]
11	Co 1D coordination polymer on carbon cloth	KOH	1.33 V vs. RHE	10	formate	77	[31]
12	PMo_{12}	PMo_{12}-acid	1.0	200	formic acid	98 for H_2	This work

Table S4 The conversions and TPA yields of PET catalyzed by common acids and PMo_{12}-acid systems.

NO.	Acid species	Acid concentration (mol L^{-1})	PMo_{12} (mol L^{-1})	Time (h)	PET conversion (%)	TPA yield (%)
1	H_2SO_4	2.5	—	10	0	0
2	H_2SO_4	4.0	—	10	0	0
3	HNO_3	2.5	—	10	0	0
4	HNO_3	4.0	—	10	11.77	8.96
5	HTOf	2.5	—	10	11.64	8.61
6	HTOf	4.0	—	10	34.56	32.07
7	$HClO_4$	2.5	—	10	0	0
8	$HClO_4$	4.0	—	10	21.96	19.87
9	HCl	2.5	—	10	0	0
10	HCl	4.0	—	10	0	0
11	PMo_{12}	—	0.1	4	0	0
12	PMo_{12}	—	0.1	10	0	0
13	PMo_{12}	—	0.5	4	11.51	8.64
14	PMo_{12}	—	0.7	4	41.05	39.34
15	PMo_{12}	—	0.93	4	83.35	81.99
16	PMo_{12}	—	0.5	10	48.22	45.97
17	PMo_{12}	—	1.0	1	44.32	42.02
18	PMo_{12}	—	1.0	2	68.45	66.89
19	PMo_{12}	—	1.0	4	90.55	89.40
20	PMo_{12}	—	1.0	6	95.05	93.88
21	PMo_{12}	—	1.0	8	97.18	96.29
22	PMo_{12}	—	1.0	10	100	98.88
23	PMo_{12}-HTOf	2.5	0.1	4	62.41	60.04
24	PMo_{12}-HTOf	2.5	0.1	10	90.20	88.10
25	PMo_{12}-$HClO_4$	2.5	0.1	4	52.26	50.04
26	PMo_{12}-$HClO_4$	2.5	0.1	10	80.91	77.45
27	PMo_{12}-H_2SO_4	2.5	0.1	4	39.22	37.52
28	PMo_{12}-H_2SO_4	2.5	0.1	10	63.03	60.43

Reaction conditions: aqueous solution 10 mL, PET 1.0 g, 100 ^{o}C.

Table S5 PET conversions and TPA yields of PET in PMo_{12}-acid (HTOf and $HClO_4$) solution with different reaction times.

NO.	Time (h)	PMo_{12} (mol L^{-1})	HTOf (mol L^{-1})	$HClO_4$ (mol L^{-1})	PET conversion (%)	TPA yield (%)
1	0.5	0.1	2.5	—	15.4	13.01
2	1	0.1	2.5	—	25.7	23.2
3	2	0.1	2.5	—	41.4	39.8
4	4	0.1	2.5	—	62.41	60.08
5	6	0.1	2.5	—	77.40	75.74
6	8	0.1	2.5	—	84.7	81.95
7	10	0.1	2.5	—	90.20	88.42
8	0.5	0.1	—	2.5	11.75	9.41
9	1	0.1	—	2.5	20.05	18.71
10	2	0.1	—	2.5	33.73	31.64
11	4	0.1	—	2.5	55.31	53.47
12	6	0.1	—	2.5	67.57	65.66
13	8	0.1	—	2.5	74.76	72.60
14	10	0.1	—	2.5	80.91	78.78

Reaction conditions: aqueous solution 10 mL, PET 1.0 g, 100 ^{o}C.

Table S6 PET conversions and TPA yields of PET in regenerated PMo_{12}-HTOf aqueous solution at different cycles.

NO.	Cycles	PMo_{12} (mol L^{-1})	HTOf (mol L^{-1})	PET conversion (%)	TPA yield (%)
1	1	0.1	2.5	94.45	91.45
2	2	0.1	2.5	93.26	90.15
3	3	0.1	2.5	92.75	90.12
4	4	0.1	2.5	91.71	89.58
5	5	0.1	2.5	91.12	88.14

Reaction conditions: aqueous solution 50 mL, PET 5 g, 100 ºC, 10 hours.

Table S7 PET conversions and TPA yields of PET in PMo_{12}-HTOf and PMo_{12}-$HClO_4$ systems with different H^+ concentrations.

NO.	Total H^+ concentration (mol L^{-1})	system	PMo_{12} (mol L^{-1})	PET conversion (%)	TPA yield (%)
1	1	PMo_{12}-HTOf	0.1	13.5	11.62
2	1.5	PMo_{12}-HTOf	0.1	32.79	30.14
3	2	PMo_{12}-HTOf	0.1	47.2	45.12
4	2.5	PMo_{12}-HTOf	0.1	62.5	60.17
5	3	PMo_{12}-HTOf	0.1	72.5	69.45
6	1	PMo_{12}-$HClO_4$	0.1	12.15	10.74
7	1.5	PMo_{12}-$HClO_4$	0.1	27.63	24.69
8	2	PMo_{12}-$HClO_4$	0.1	39.78	37.54
9	2.5	PMo_{12}-$HClO_4$	0.1	55.31	53.01
10	3	PMo_{12}-$HClO_4$	0.1	65.27	63.52

Reaction conditions: aqueous solution10 mL, PET 1.0 g, 100 ^{o}C, 4 hours.

Table S8 PET conversions and TPA yields of PET in PMo_{12}-HTOf and PMo_{12}-$HClO_4$ aqueous solutions under different PMo_{12} concentrations.

NO.	PMo_{12} concentration (mol L^{-1})	system	H^+ total concentration (mol L^{-1})	PET conversion (%)	TPA yield (%)
1	0.025	PMo_{12}-HTOf	2.8	17.2	14.5
2	0.05	PMo_{12}-HTOf	2.8	46.94	44.56
3	0.075	PMo_{12}-HTOf	2.8	57.6	54.78
4	0.1	PMo_{12}-HTOf	2.8	62.41	60.04
5	0.125	PMo_{12}-HTOf	2.8	66.75	64.66
6	0.15	PMo_{12}-HTOf	2.8	69.66	67.25
7	0.025	PMo_{12}-$HClO_4$	2.8	1.20	0
8	0.05	PMo_{12}-$HClO_4$	2.8	32.90	30.72
9	0.075	PMo_{12}-$HClO_4$	2.8	42.65	40.45
10	0.1	PMo_{12}-$HClO_4$	2.8	55.31	54.07
11	0.125	PMo_{12}-$HClO_4$	2.8	59.53	58.01
12	0.15	PMo_{12}-$HClO_4$	2.8	64.37	61.99

Reaction conditions: aqueous solution 10 mL, H_3PO_4 0.8 mol L^{-1}, PET 1.0 g, 100 ^oC, 4 hours.

Table S9 PET conversions and TPA yields of PET in PMo_{12} aqueous solution with different reaction times and different temperatures.

NO.	Temperature (°C)	Time (h)	PMo_{12} (mol L^{-1})	PET conversion (%)	TPA yield (%)
1	100	1	1.0	44.32	42.02
2	100	2	1.0	68.45	66.89
3	100	4	1.0	90.55	89.40
4	100	6	1.0	95.05	93.88
5	90	1	1.0	26.91	25.02
6	90	2	1.0	53.22	51.23
7	90	4	1.0	72.42	70.95
8	90	6	1.0	82.87	80.87
9	80	1	1.0	9.76	7.82
10	80	2	1.0	31.32	30.05
11	80	4	1.0	49.85	47.49
12	80	6	1.0	60.25	58.78

Reaction conditions: aqueous solution 10 mL, PET 1.0 g.

Table S10 PET conversions and TPA yields of PET in PMo_{12}-HTOf aqueous solution with different times and different temperatures.

NO.	Temperature (°C)	Time (h)	PMo_{12} (mol L^{-1})	PET conversion (%)	TPA yield (%)
1	100	2	0.1	41.41	39.8
2	100	4	0.1	62.41	60.08
3	100	6	0.1	77.40	75.74
4	100	8	0.1	84.73	81.95
5	90	2	0.1	16.62	15.51
6	90	4	0.1	32.74	30.71
7	90	6	0.1	44.75	43.15
8	90	8	0.1	54.26	53.12
9	80	2	0.1	7.26	5.24
10	80	4	0.1	18.45	17.02
11	80	6	0.1	30.52	28.97
12	80	8	0.1	38.65	36.45
13	70	2	0.1	5.32	4.75
14	70	4	0.1	11.95	11.01
15	70	6	0.1	18.65	16.45
16	70	8	0.1	23.04	21.42

Reaction conditions: aqueous solution 10 mL, HTOf 2.5 mol L^{-1}, PET 1.0 g.

Table S11 PET conversions and TPA yields of PET hydrolysis in regenerated PMo_{12}-HTOf and H_3PO_4 aqueous solution at different cycles.

NO.	Cycles	PMo_{12} (mol L^{-1})	HTOf (mol L^{-1})	H_3PO_4 (mol L^{-1})	PET conversion (%)	TPA yield (%)
1	1	0.1	2.5	0.8	93.15	88.99
2	2	0.1	2.5	0.8	92.25	90.52
3	3	0.1	2.5	0.8	92.04	89.78
4	4	0.1	2.5	0.8	93.45	90.39
5	5	0.1	2.5	0.8	94.66	91.03
6	6	0.1	2.5	0.8	92.42	90.37
7	7	0.1	2.5	0.8	90.64	87.56
8	8	0.1	2.5	0.8	91.33	89.44
9	9	0.1	2.5	0.8	89.03	87.91
10	10	0.1	2.5	0.8	92.28	88.86

Reaction conditions: aqueous solution 50 mL, PET 5.0 g, 10 hours, 100 ^{o}C.

Table S12 PET conversions and TPA yields of PET in regenerated PMo_{12}-H_2SO_4 and H_3PO_4 aqueous solution at different cycles.

NO.	Cycles	PMo_{12} (mol L^{-1})	H_2SO_4 (mol L^{-1})	H_3PO_4 (mol L^{-1})	PET conversion (%)	TPA yield (%)
1	1	0.1	2.5	0.8	66.41	64.23
2	2	0.1	2.5	0.8	65.29	63.25
3	3	0.1	2.5	0.8	66.02	64.09
4	4	0.1	2.5	0.8	65.74	63.27
5	5	0.1	2.5	0.8	64.52	62.78
6	6	0.1	2.5	0.8	64.96	61.07
7	7	0.1	2.5	0.8	65.36	63.68
8	8	0.1	2.5	0.8	63.25	61.27
9	9	0.1	2.5	0.8	63.49	61.17
10	10	0.1	2.5	0.8	63.04	60.5

Reaction conditions: aqueous solution 50 mL, PET 5.0 g, 10 hours, 100 ^{o}C.

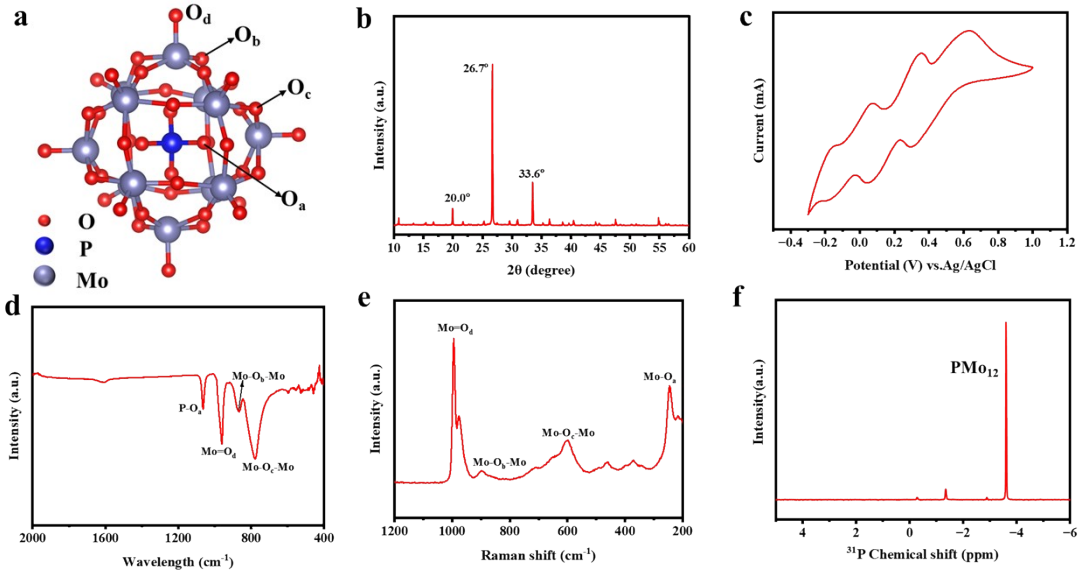

Fig. S1 (a) Structure illustration, (b) the XRD pattern, (c) Cyclic voltammetry curve, (d) FT-IR spectrum, (e) Raman spectrum and (f) ^{31}P NMR spectrum of PMo_{12}.

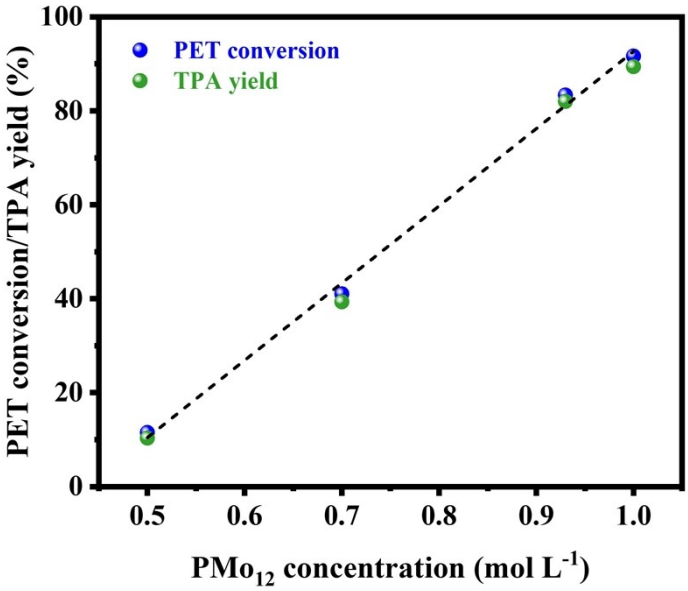

Fig. S2 PET conversions and TPA yields of PET hydrolysis reaction in PMo_{12} aqueous solution with different PMo_{12} concentrations (Reaction conditions: PMo_{12} aqueous solution 10 mL, PET 1.0 g, 100 ^{o}C, 4 hours).

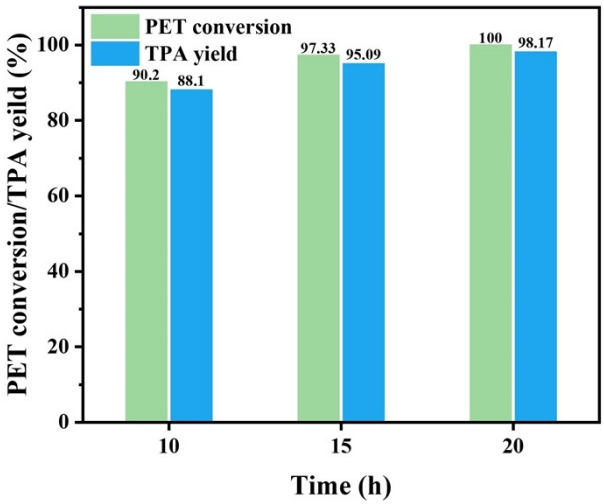

Fig. S3 Conversions of PET in PMo_{12}-HTOf systems with different reaction times (Reaction conditions: aqueous solution 10 mL, PMo_{12} 0.1 mol L^{-1} and HTOf 2.5 mol L^{-1}, PET 1.0 g, 100 ^{o}C).

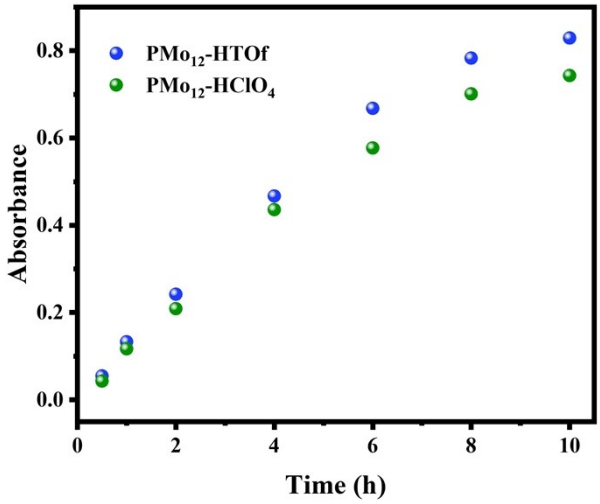

Fig. S4 Absorbances of PMo_{12}-HTOf and PMo_{12}-$HClO_4$ solutions after reacting with PET at different reaction times. After each reaction, a certain amount of filtered reaction solution was diluted to a PMo_{12} concentration of 10 mmol L^{-1}, and the absorbance was measured at the wavelength of 750 nm.

Fig. S5 Photo images of produced TPA by different cyclic reactions.

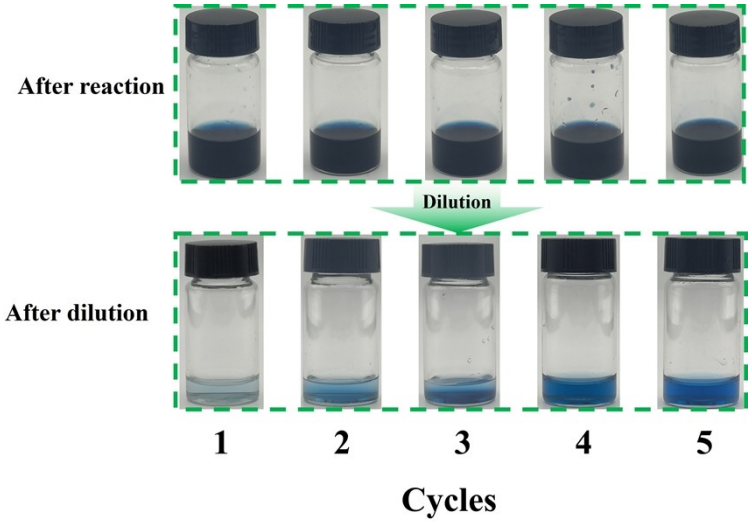

Fig. S6 Photo images of reaction solutions after different cycles. After each reaction, 5 mL of the filtered reaction solution was put into a small bottle and diluted to the PMo_{12} concentration of 1 mmol L^{-1}.

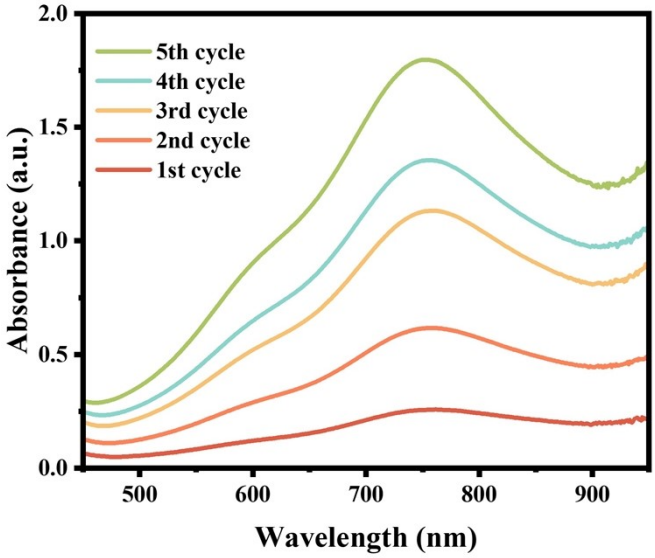

Fig. S7 UV-Vis spectra of PMo_{12}-HTOf reaction solutions with different cycles (after the reaction, the solution was diluted to 1 mmol L^{-1} of PMo_{12}).

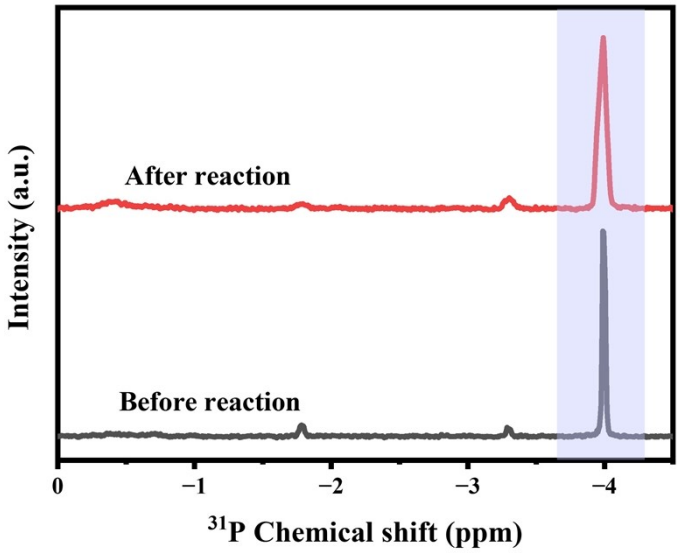

Fig. S8 ^{31}P NMR spectra of PMo_{12}-HTOf solution before and after reaction. The signal near 3.9 ppm (^{31}P NMR) can be assigned to PMo_{12}.[32]

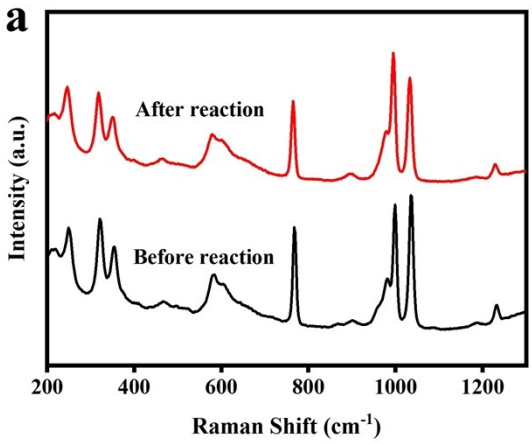

b

Species	Raman shift (cm^{-1})
Vs(Mo=Ot)	1010/996
Vas(Mo-Ot)	967
Vs(Mo-Ob-Mo)	908
Vs(Mo-Oc-Mo)	610
Vs(Mo-Oa)	250

Fig. S9 (a) Raman spectra of PMo_{12}-HTOf solution before and after reaction. (b) Summary of Raman shifts corresponding to different bonds of PMo_{12}.[32]

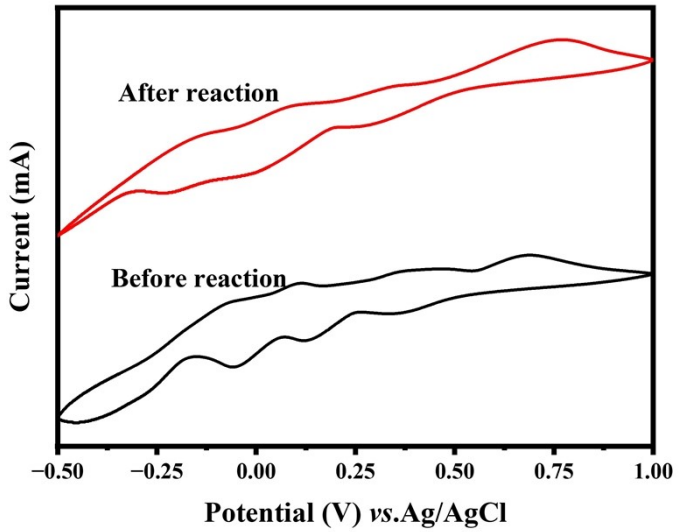

Fig. S10 Cyclic voltammetry curves of PMo_{12}-HTOf solutions before and after reaction on graphite electrode (0.157 cm^2) with scan rate 50 mV s^{-1} at 25 ºC.

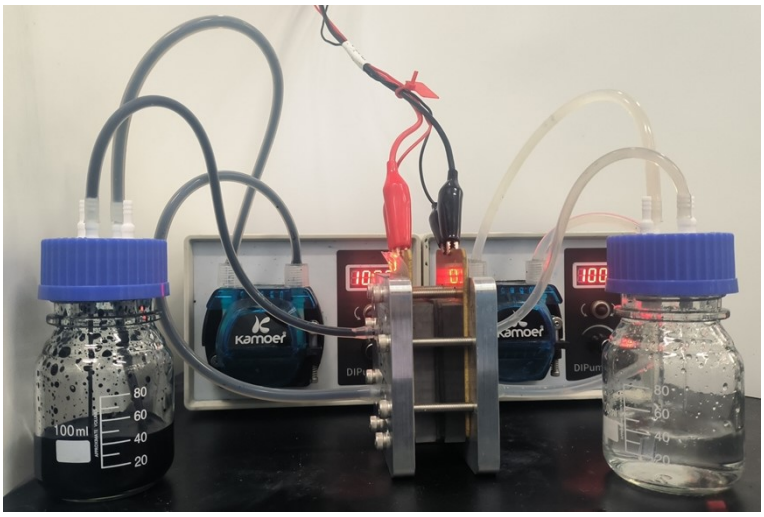

Fig. S11 The experimental image for electrolytic regeneration of reduced PMo_{12} and cathodic hydrogen production in a proton exchange membrane electrolysis cell (PEMEC).

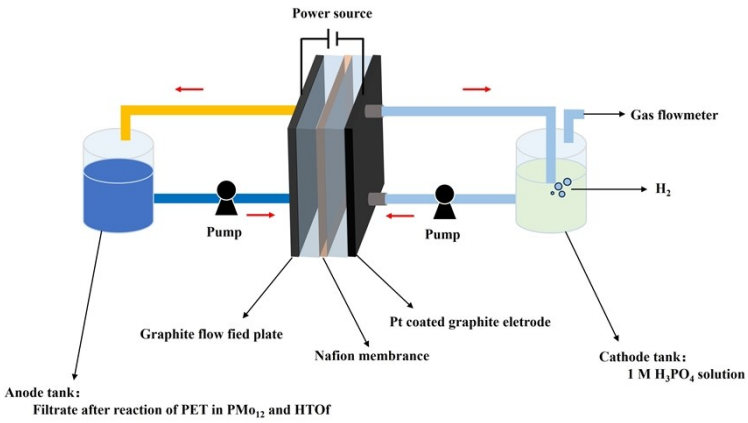

Fig. S12 Experimental set-up for electrolytic regeneration of reduced PMo_{12} and cathode hydrogen production in a proton exchange membrane electrolysis cell (PEMEC).

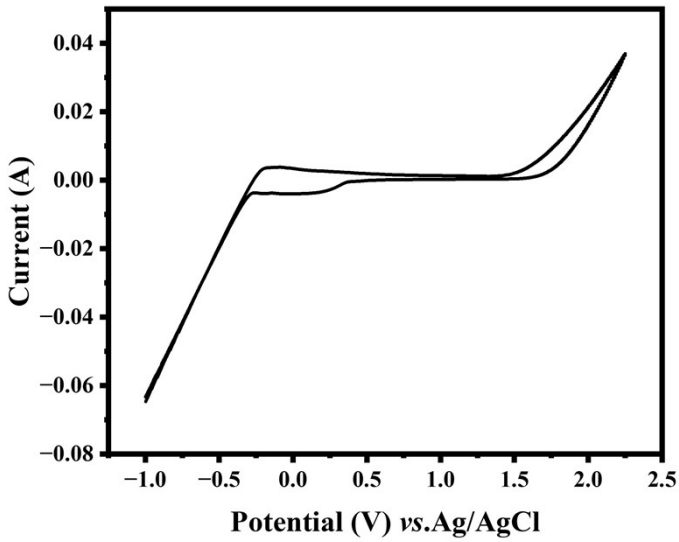

Fig. S13 Cyclic voltammetry curve of H_3PO_4 solution (1 mol L^{-1}) on graphite electrode with scan rate 50 mV s^{-1} at 25 ºC.

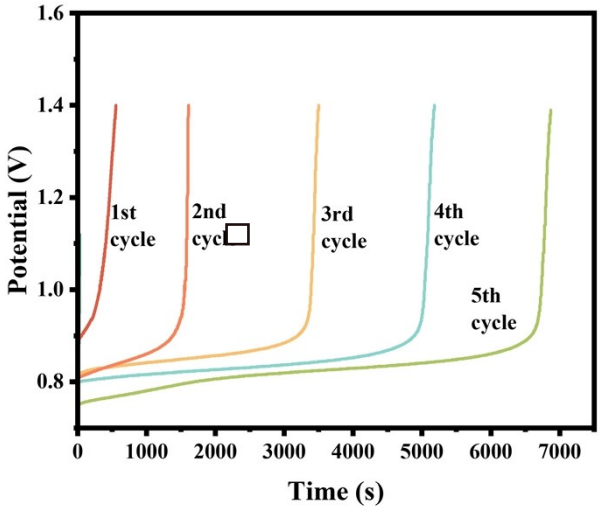

Fig. S14 Applied potential-times curves of solution at different electrolytic regeneration cycles in PEMEC with constant current density (50 mA cm^{-2}; electrode area: 1cm^2).

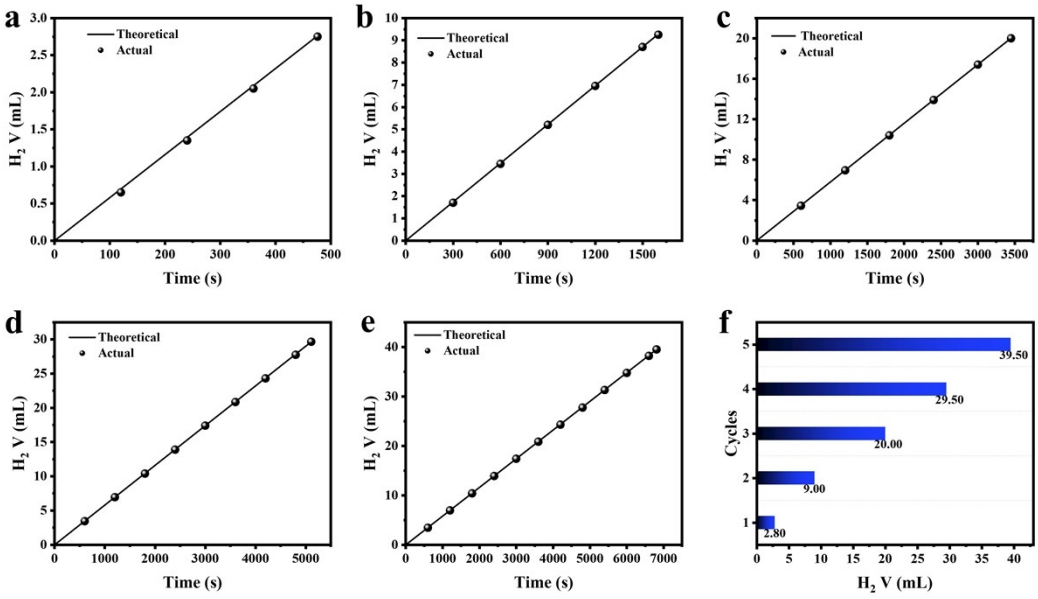

Fig. S15 Volumes of actual produced H_2 compared with theoretically calculated H_2 volumes assuming a 100% Faradaic efficiency in the cathodic H_2 evolution. Theoretical H_2 = (total charge during potentiostatic electrolysis) × 2/F, where F is the Faraday constant (96485 C mol^{-1}).

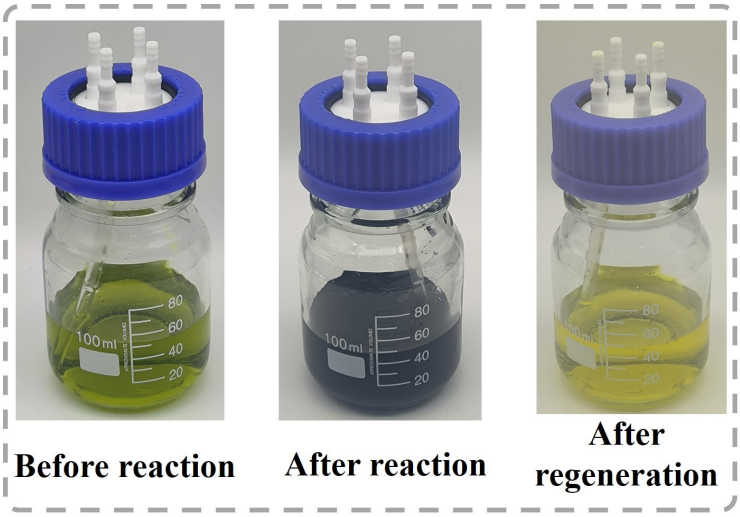

Fig. S16 Images of PMo_{12}-HTOf solution before reaction, after reaction with PET, and after electrolytic regeneration.

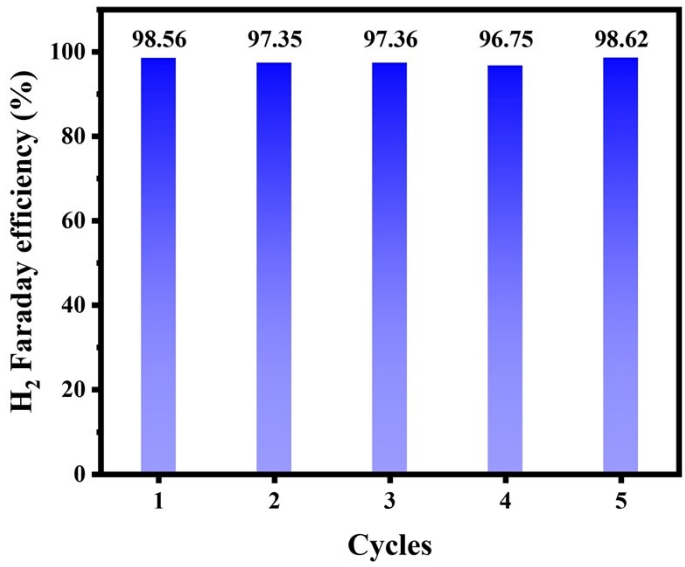

Fig. S17 Faraday efficiency of hydrogen production by electrolysis of reaction solutions at different cycles.

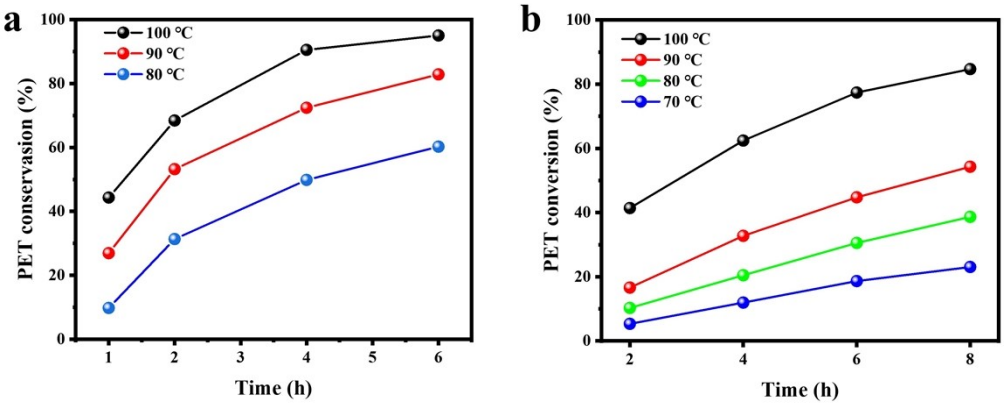

Fig. S18 PET conversions in (a) PMo_{12}-HTOf and (b) pure PMo_{12} aqueous solution with different times and different temperatures.

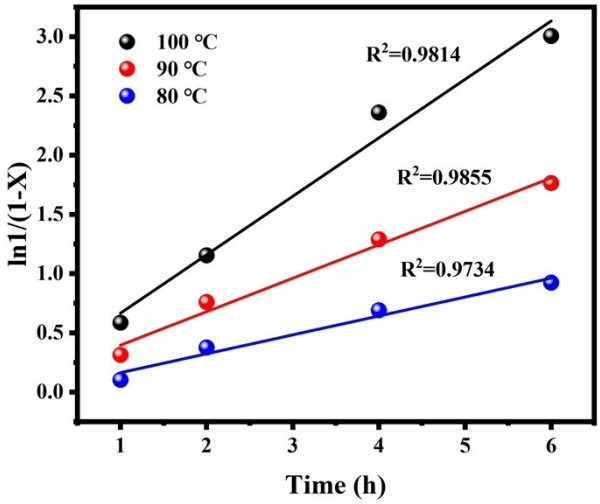

Fig. S19 Plots of ln1/(1-x) vs. PET degradation time with pure PMo_{12} at 80 °C, 90 °C and 100 °C, respectively.

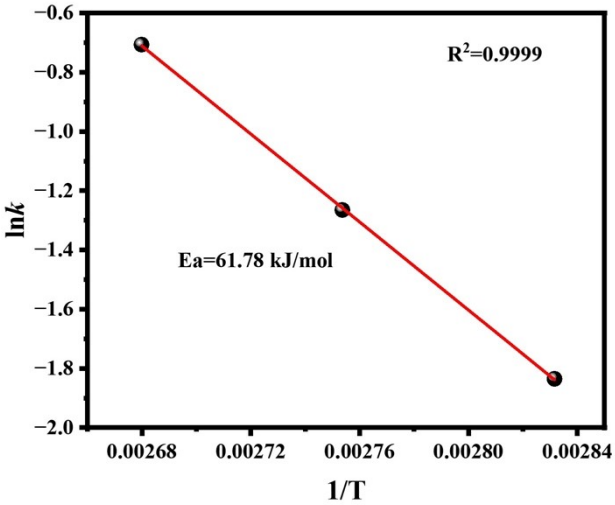

Fig. S20 Arrhenius plots of the rate constant of PET hydrolysis with PMo_{12}.

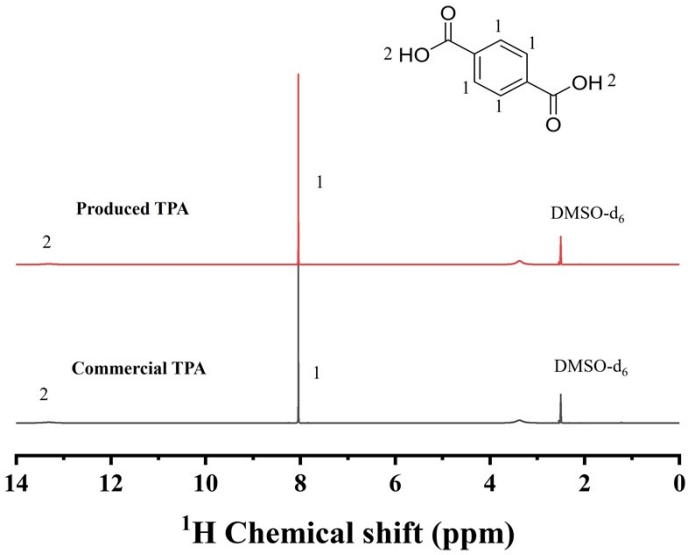

Fig. S21 ^{1}H NMR of commercial TPA and the TPA obtained from this study. The same amount of commercial TPA and product TPA were added into DMSO-d6 solvent for ^{1}H NMR measurements (500 Hz).[4]

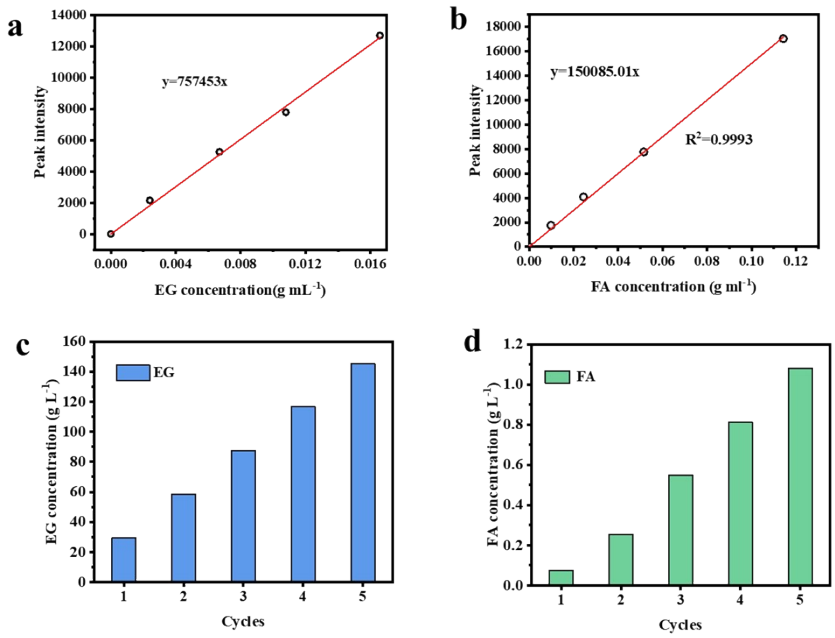

Fig. S22 Calibration curves for (a) EG and (b) FA solution by ^{1}H NMR. The calculated concentrations of (c) EG and (FA) in the reaction solution after different reaction cycles.

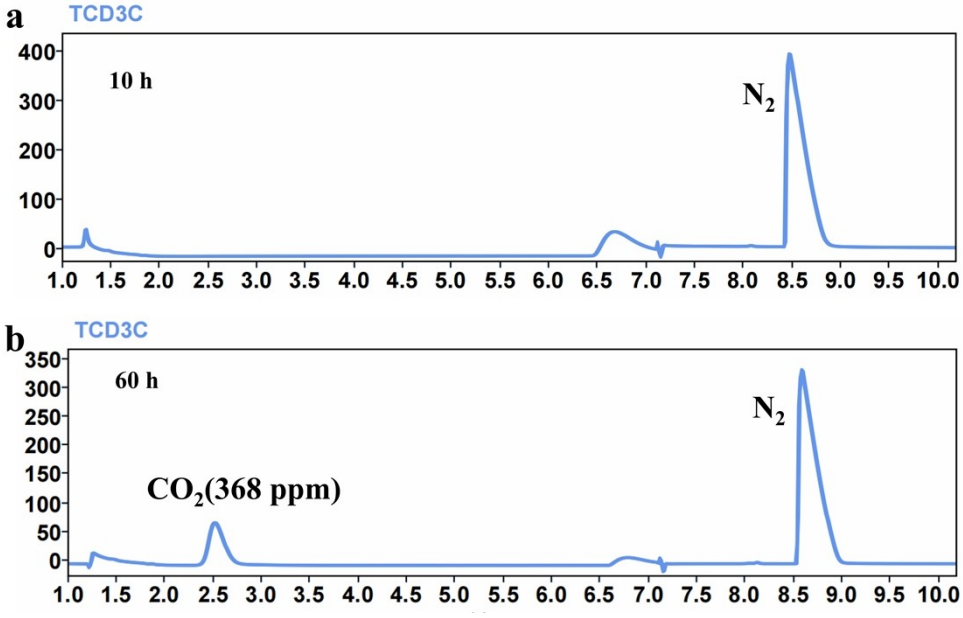

Fig. S23 Gas emission measurement of PMo_{12}-HTOf solution with PET after reaction for (a) 10 h and (b) 60 h.

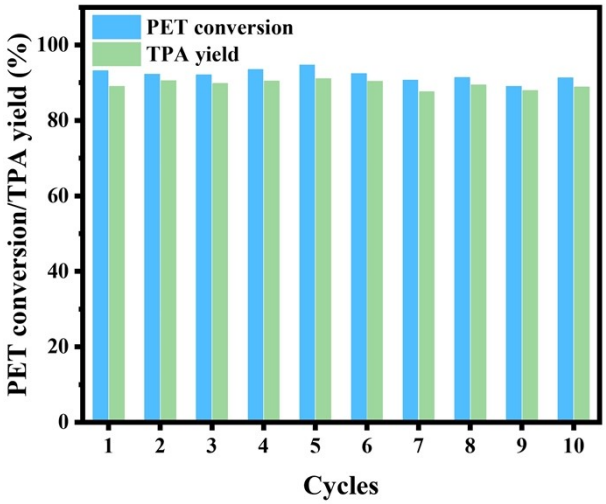

Fig. S24 PET conversions in regenerated PMo_{12}-HTOf aqueous solution at different cycles (Reaction conditions: aqueous solution 50 mL, PET 5.0 g, PMo_{12} 0.1 mol L^{-1} and HTOf 2.5 mol L^{-1}, H_3PO_4 0.8 mol L^{-1}, 10 hours, 100 ^{o}C).

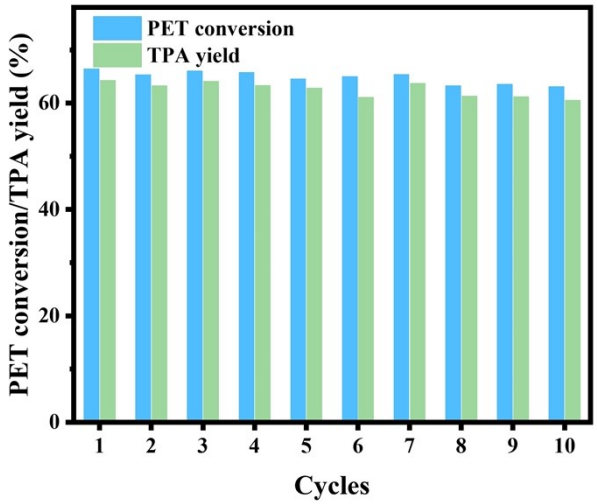

Fig. S25 PET conversions in regenerated PMo_{12}-H_2SO_4 aqueous solution at different cycles (Reaction conditions: aqueous solution 50 mL, PET 5.0 g, PMo_{12} 0.1 mol L^{-1} and H_2SO_4 2.5 mol L^{-1}, H_3PO_4 0.8 mol L^{-1}, 10 hours, 100 ^{o}C).

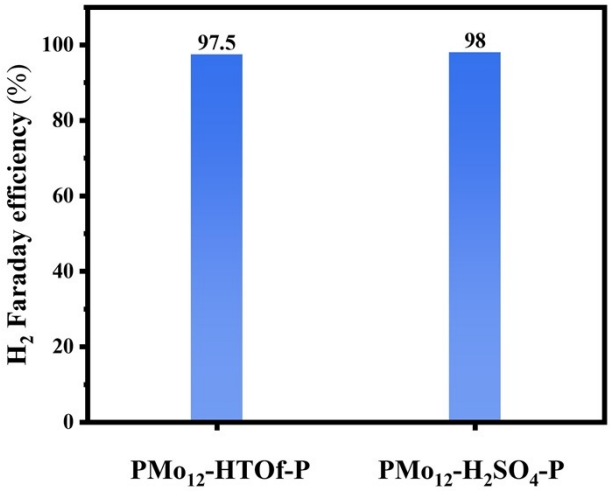

Fig. S26 Faraday efficiency of hydrogen production from solution electrolysis after PET reaction with PMo_{12}-H_2SO_4 (and PMo_{12}-HTOf) and 0.8 mol L^{-1} H_3PO_4 solution.

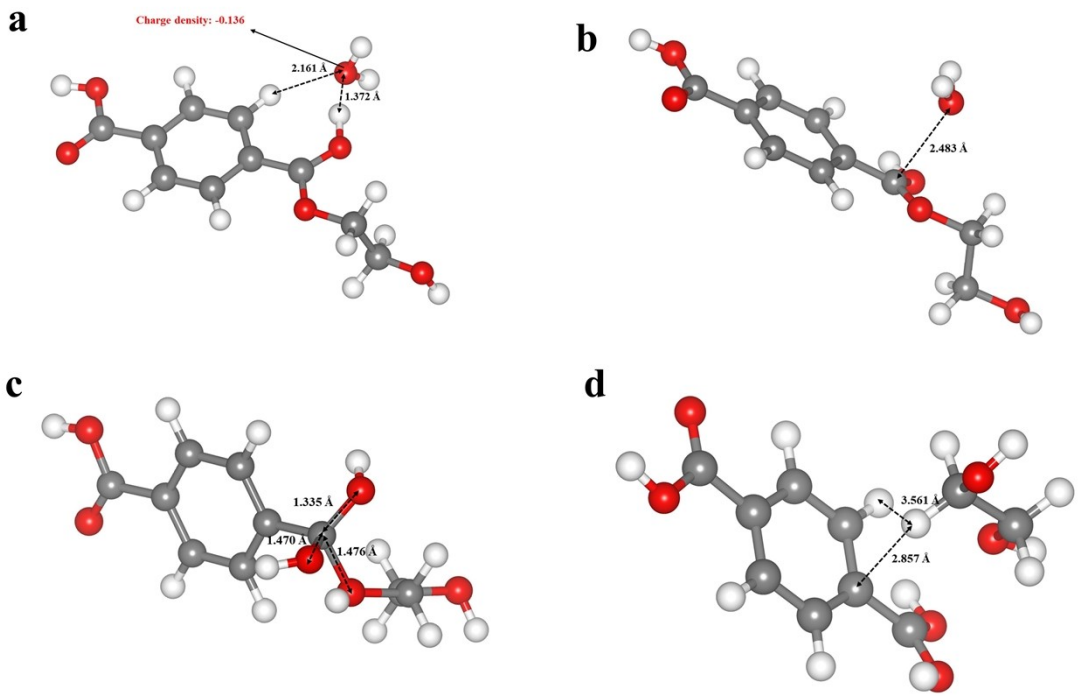

Fig. S27 Optimized molecular configuration in traditional acidic hydrolysis reaction of PET monomer by DFT. (a) Protonation of glycol terephthalate. (b) Glycol terephthalate attacking by a water molecule. (c) The transition state of glycol terephthalate during hydrolysis. (d) TPA and ethylene glycol molecules after completion of hydrolysis.

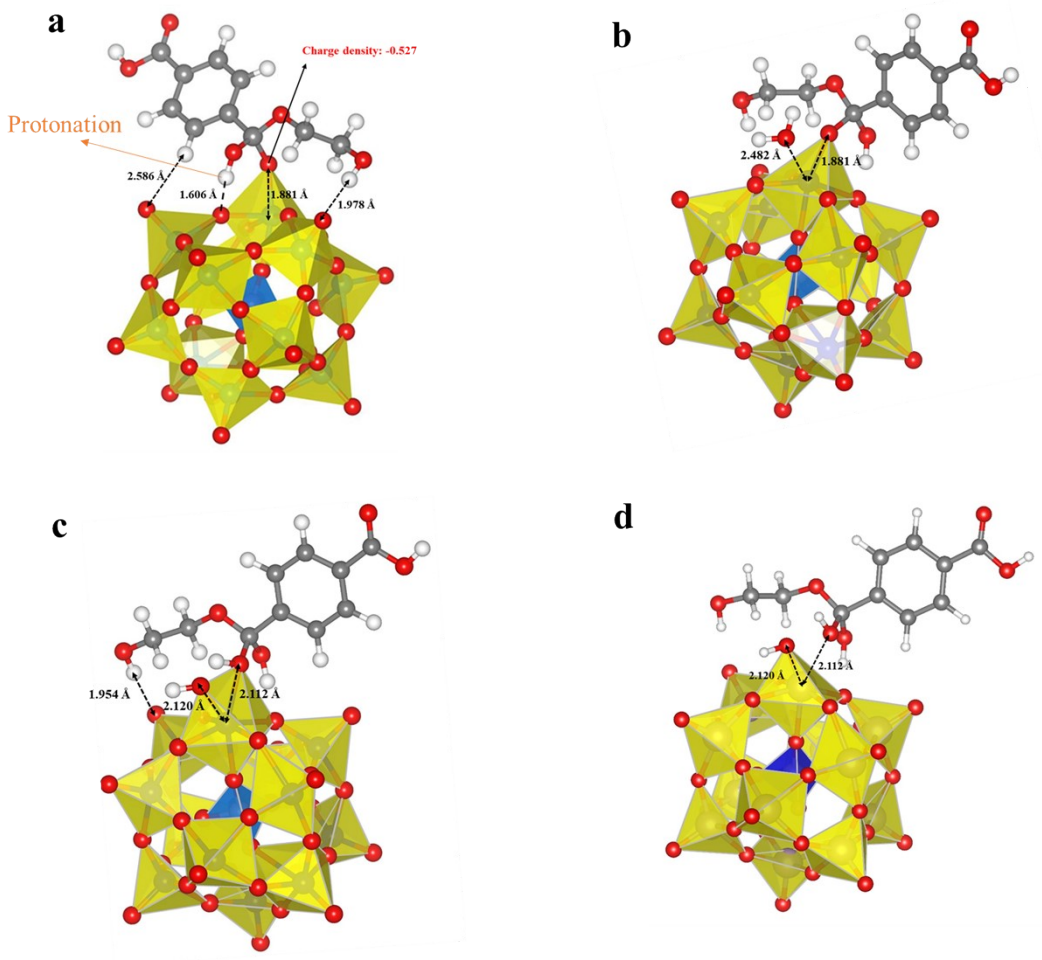

Fig. S28 Optimized molecular configuration in PMo_{12} catalyzed hydrolysis reaction of PET monomer by DFT. (a) Adsorption of protonated glycol terephthalate on PMo_{12}. (b) Glycol terephthalate attacking by O_d of PMo_{12}. (c) The transition state of glycol terephthalate catalyzed by PMo_{12} during hydrolysis. (d) Completion of glycol terephthalate hydrolysis with the PMo_{12} catalyst.

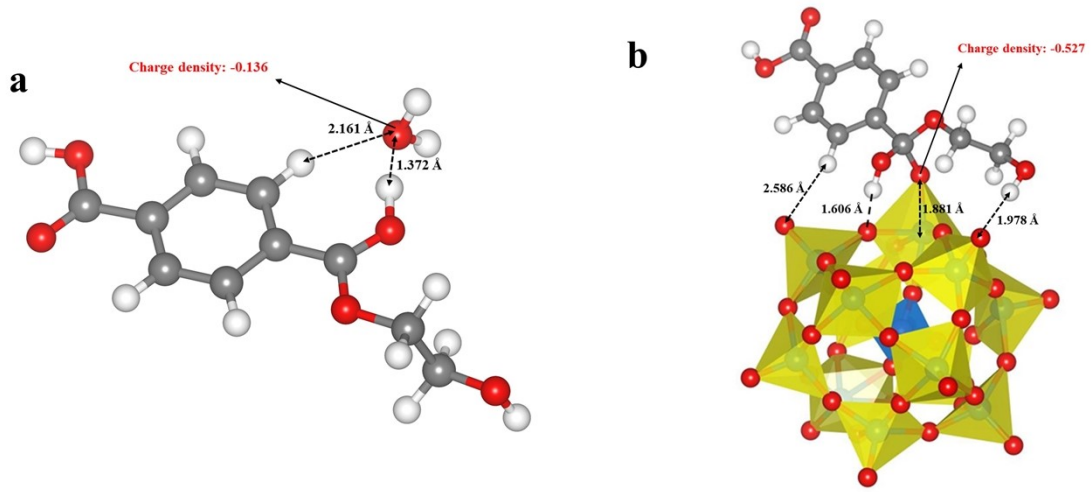

Fig. S29 The charge densities of the (a) O in water and (b) O_d in PMo_{12} when attacking the carbonyl carbon atom of the ester group.

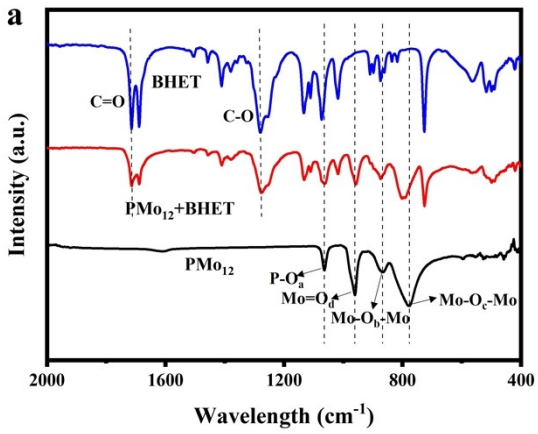

b

	PMo_{12}	PMo_{12}+PET	PMo_{12}+BHET
P-O_a	1063.3	1060.5	1060.5
Mo=O_d	960.1	962.9	955.8
Mo-Ob-M_o	865.3	872.5	874.0
Mo-O_c-Mo	777.8	786.4	789.3

c

	PET	PMo_{12}+PET	BHET	PMo_{12}+BHET
C=O	1714.9	1713.4	1714.9	1713.4
C-O	1241.3	1239.9	1280.0	1272.9

Fig. S30 (a) FT-IR spectra of Bis (2-hydroxyethyl) terephthalate (BHET) model compound mixed with PMo_{12}. The PMo_{12}+BHET samples were prepared by simply grounding BHET with PMo_{12} at a ratio of 5:1 (mol/mol). (b) Summary of the FT-IR absorption peaks of P-O_a, Mo-O_b-Mo, Mo-O_c-Mo, Mo=O_d. (c) Summary of the FT-IR absorption peaks of C=O, C-O bond. It was found that the FT-IR absorption peaks of P-O_a, Mo-O_b-Mo, Mo-O_c-Mo and Mo=O_d shifted after the adsorption of PMo_{12} with BHET, which was consistent with the DFT calculated results. The blue shift of the C=O, C-O bond can be detected.

a

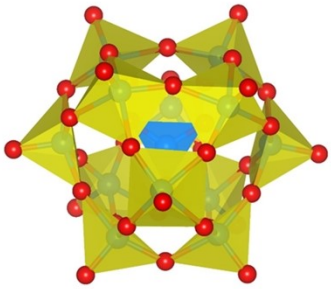

PMo_{12}

	Bond length
P-O_a	1.570 Å
Mo-O_b-Mo	1.823 Å
Mo-O_c-Mo	2.025 Å
Mo=O_d	1.695 Å

b

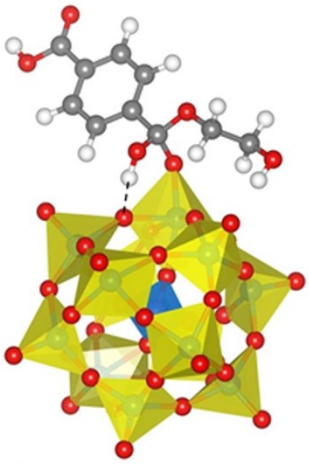

	Bond length
P-O_a	1.477 Å
Mo-O_b-Mo	1.927 Å
Mo-O_c-Mo	2.070 Å
Mo=O_d	1.882 Å

Adsorption of protonated glycol terephthalate on PMo_{12}

Fig. S31 (a) The bond length of Mo-O_b-Mo, Mo-O_c-Mo and Mo=O_d in PMo_{12} optimized by DFT structure. (b) The bond length of Mo-O_b-Mo, Mo-O_c-Mo and Mo=O_d of PMo_{12} after adsorption of ethylene terephthalate was optimized by DFT structure.

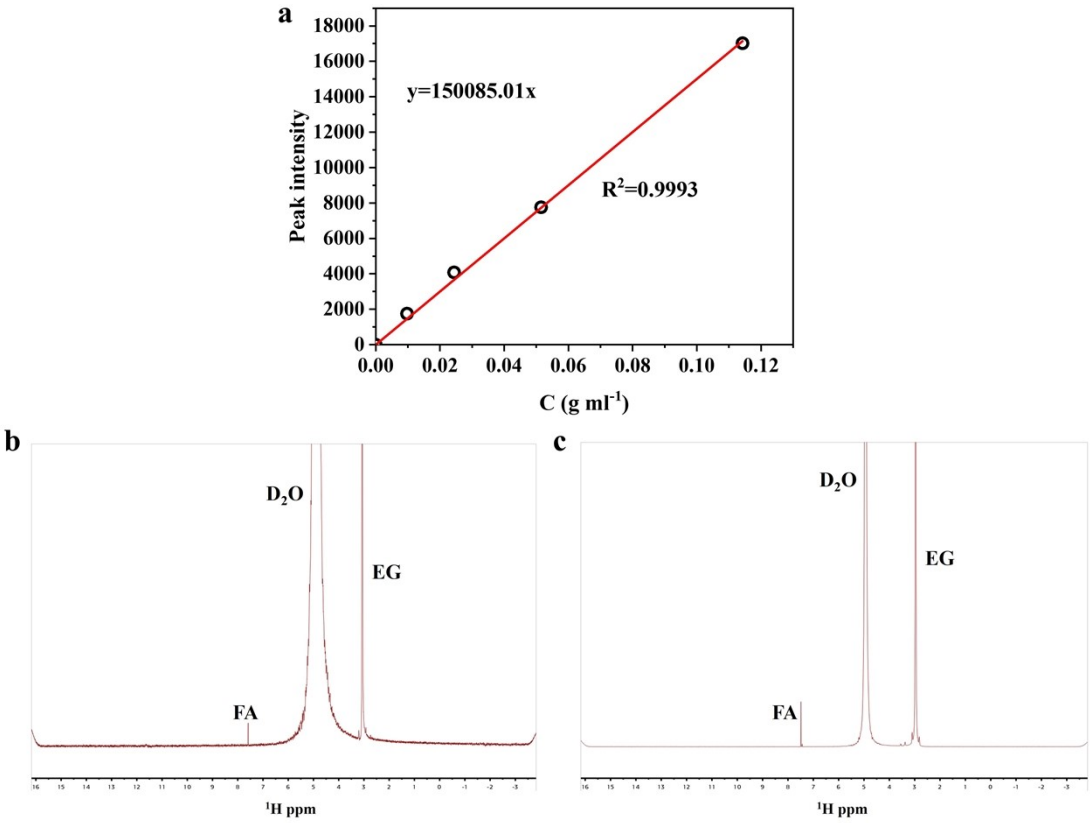

Fig. S32 (a) Calibration curve for FA solution with different concentrations by ^{1}H NMR. ^{1}H NMR spectra of the PMo_{12}-HTOf solution after reaction with (b) 0.1 mol L^{-1} and (c) 3 mol L^{-1} EG.

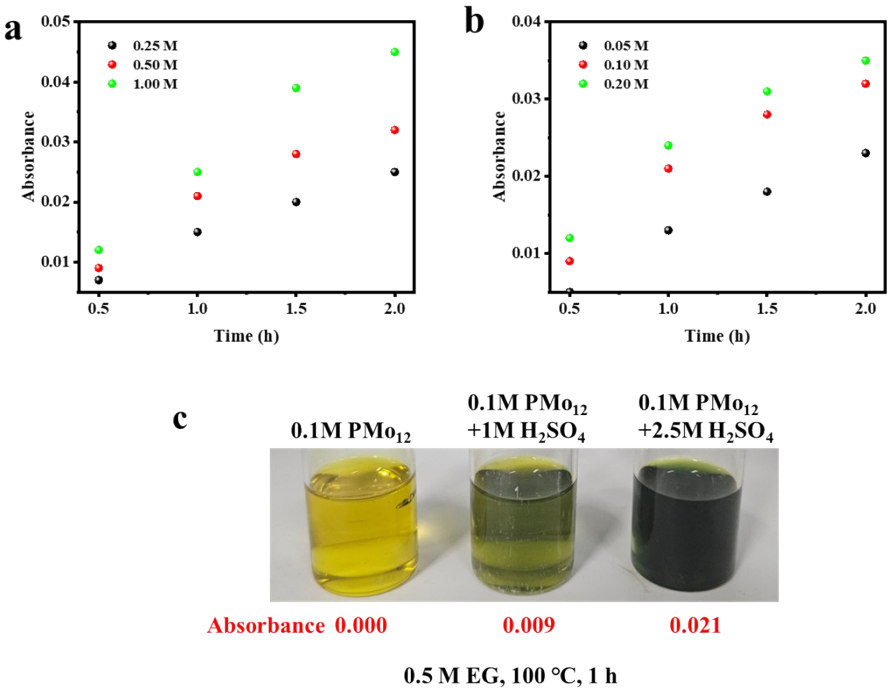

Fig. S33 Oxidation rates of EG in PMo_{12}-H_2SO_4 with different concentration of (a)EG, (b) PMo_{12} and (c) H^+

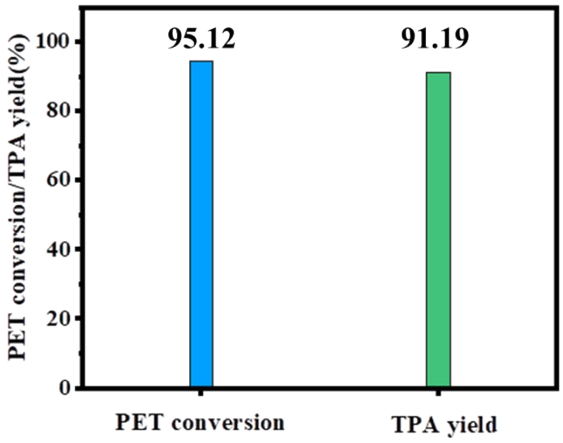

Fig.S34 PET conversion and TPA yield of PET hydrolysis in PMo_{12}-H_2SO_4 aqueous solution after 15 hrs reaction time.

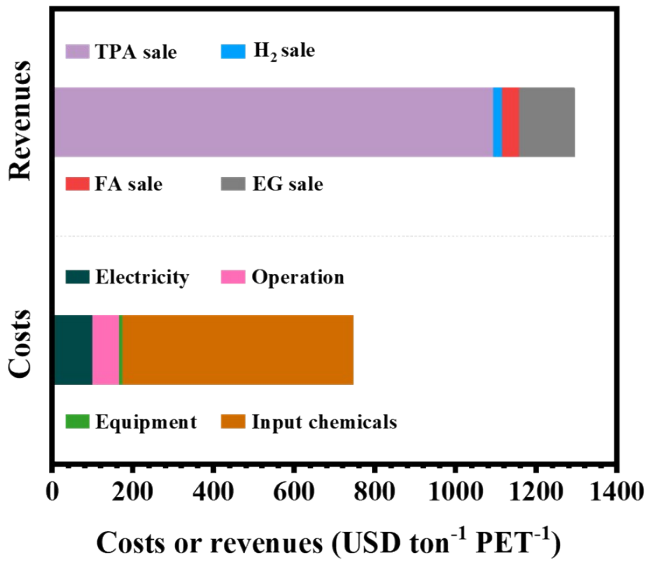

Fig. S35 Techno-economic analysis of electrolytic upcycling of PET waste plastics with hydrogen evolution catalyzed by PMo_{12}-acids system in this study.

Note S1 Process details and descriptions of ASPEN and Life-cycle assessment

1. Process details and descriptions in ASPEN.

In this simulation, as shown in **Fig. S36**, the NRTL-HOC physical property method was chosen to address the simulation process of PET acidic hydrolysis. The PET pellets were mixed with acid aqueous solution before entering the tank reactor (represented by RSTOIC). The depolymerization process was conducted at a temperature of 100 °C and a pressure of 1 atm. Subsequently, the resulting material underwent cooling and filtration in order to separate the solid TPA. The liquid phase was then directed into the electrolyzer (I=800 A, U=156 V, P=125 kW, number of electrode plates=164, area=1 m^2), which is not depicted in ASPEN. The PMo_{12} was oxidized at the anode and hydrogen was produced at the cathode.

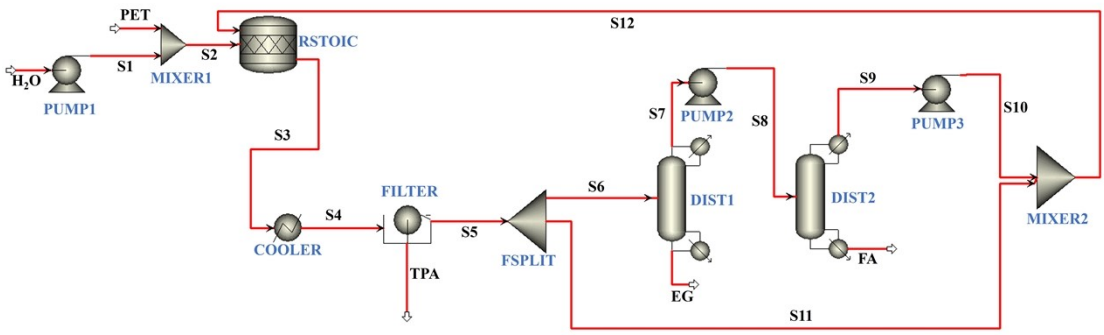

Fig. S36 Aspen Plus process flow chart of the waste PET hydrolysis.

2. Life-cycle assessment conditions.

The goal and scope definition of the LCA study conducted in this work are outlined in **Table S14**. Furthermore, the system boundary of the LCA was defined as "cradle to gate". The distribution principle of the LCA adhered to the "cut-off" rule. For the inventory analysis, the material balance and energy balance were derived from actual experimental results and Aspen simulation data. These are “prospective processes”, and the functional unit was set at 1 kg of TPA. The impact assessment was performed using the professional software OpenLCA 2.0.3, employing IPCC 2021 for GWP and CML-IA baseline for NREU as the assessment methods. Data on the "background processes" were obtained from the Ecoinvent V.3.9.1 database. **Table S15** provides the carbon footprint analysis associated with electricity, cooling water, and chemical raw materials, including their reference sources. Our LCA study addressed the greenhouse effect and achieved carbon reduction goals, with particular focus on non-renewable energy use (NREU) and Global Warming Potential (GWP).

3. ASPEN and Life-cycle assessment parameters and results.

Table S13 Utility of modules.

Modules	Type of utility	Quantity	Unit	Function
RSTOIC	U-1*	202.91	t/h	Cool the reaction tank
PUMP1	Electricity	0.3547	kW	Increase the pressure of water
COOLER	U-1*	45.02	t/h	Cool the product fluid
PUMP2	Electricity	0.019	kW	Increase the pressure
PUMP3	Electricity	0.005	kW	Increase the pressure
DIST1	U-2**	69.12	t/h	Cool the top fraction
	Electricity	292.85	kW	Heat the tower kettle
DIST2	U-2**	146.03	t/h	Cool the top fraction
	Electricity	103.75	kW	Heat the tower kettle
FILTER	Electricity	1.63	kW	Solid-liquid separation
ELECTROLYZER***	Electricity	125	kW	Reduction of PMo_{12} and hydrogen production

*Initial state of U-1: 20 ^{o}C, 1atm liquid phase. Final state of U-1: 90 ^{o}C, 1atm liquid phase.

**Initial state of U-2: 20 ^{o}C, 1atm liquid phase. Final state of U-1: 25 ^{o}C, 1atm liquid phase.

***ELECTROLYZER with voltage of 156 V, power of 125 kW and number of bipolar plates of 164.

Table S14 Goal and scope definition of this LCA study.

Goal	
Reason for conducting the study	1. This ex-ante LCA study will focus on carbon dioxide emissions and fossil energy consumption. 2. To assess the global warming potential (GWP) and Non-renewable energy use (NREU) of recycling PET bottles via acidic hydrolysis
Application	Provide technical and theoretical support for carbon emission reduction policies and circular economy.
Audience	Industrial stakeholders, the research community, and the public.
The intention of using results in a comparative study	The results are to be compared and disclosed to the public through this article publication.
Scope	
Product system	Acidic hydrolysis of waste PET produces TPA, EG, FA and H_2 catalyzed by PMo_{12}-acid system.
Functional unit	1 kg purified TPA
System boundary	Cradle to gate.
Allocation	Economic allocation.
Assumptions	1. This system is located in European countries or China. 2. An estimated annual degradation of 5700 metric tons of PET.
Requirements on data and quality	The foreground data is derived from Aspen plus V14 simulation data, and the background data is obtained based on the Ecoinvent V.3.9.1 database in Open LCA 2.0.3, to meet the requirements of technical and regional representativeness.
LCIA methodology	IPCC 2021 for GWP; CML-IA baseline for NREU.
Impact categories assessed in the study	1. Global Warming Potential (GWP, 100a), kg CO_2 equivalent. 2. Non-renewable energy use (NREU), MJ.
Limitations	Except for the assumptions mentioned above, the environmental impacts of factory construction and equipment maintenance have not been included in the calculation.
Report requirements	To present the outcome via journal publication which is openly accessible to everyone.

Table S15 Cradle-to-gate LCA results of hydrolysis post-consumer PET, functional unit = 1 kg TPA.

Process	Based on the background data from China		Based on the background data from Europe	
	NREU (MJ kg^{-1} TPA)	**GWP* (kg CO_2-eq kg^{-1} TPA)**	**NREU (MJ kg^{-1} TPA)**	**GWP* (kg CO_2-eq kg^{-1} TPA)**
1. PET bottles to flakes	7.22	0.71	5.42	0.43
1.1 Collection	0.24	0.024	0.18	0.0133
1.2 Transportation	1.38	0.12	0.77	0.05
1.3 Grinding and washing	5.59	0.57	4.47	0.36
2. PET flakes to pellets	2.94	0.32	1.56	0.13
3. PET pellets to TPA	5.7	0.63	2.70	0.23
Total	15.85	1.66	9.72	0.80

*The GWP was calculated based on economic values of the product TPA (TPA: 1.26 USD kg^{-1}, H_2: 1.9 USD kg^{-1}, EG: 0.64 USD kg^{-1}, FA (70%): 0.21 USD kg^{-1}).

Table S16 Compared data from Ecoinvent 3.9.1 database.

Item	GWP (kg CO_2-eq kg^{-1} TPA)	NREU (MJ kg^{-1} TPA)
Purified terephthalic acid production (rest of world*)	2.00	49.81
Purified terephthalic acid production (Europe)	1.80	48.06

*The rest of the world represents China.

Table S17 Input-output of Mechanical shredding PET bottles to flakes, functional unit = 1 kg PET flakes*.

Item	Quantity	Unit	Ref.
Input			
PET baled bottles	1316	kg	[33]
Electricity	447	kw·h	[33]
Heat from natural gas	2500	MJ	[33]
NaOH (30%)	10	kg	[33]
Sulfuric acid (30%)	20	kg	[33]
Transportation	300	km	Assumption
Output			
By-products (e.g. PE)	88	kg	[33]
Solid waste	222	kg	[33]
PET flakes	1000	kg	[33]

*Calculation results: Based on the background data from China: NREU 7.22 MJ kg^{-1} PET flakes; GWP 0.7089 kg CO_2-eq kg^{-1} PET flakes. Based on the background data from Europe: NREU 5.42 MJ kg^{-1} PET flakes; GWP 0.4328 kg CO_2-eq kg^{-1} PET flakes.

Table S18 Input-output of PET flakes to pallet, functional unit = 1 kg PET pellets*.

Item	Quantity	Unit	Ref.
Input			
PET flakes	1031	kg	[33]
Electricity (pellet extrusion)	278	kw·h	[33]
The heat from natural gas	252	MJ	[33]
Output			
Solid waste	31	kg	[33]
PET pellets	1000	kg	[33]

*Calculation results: Based on the background data from China: NREU 2.94 MJ kg^{-1} PET pellets; GWP 0.3231 kg CO_2-eq kg^{-1} PET pellets. Based on the background data from Europe: NREU 1.56 MJ kg^{-1} PET pellets; GWP 0.1343 kg CO_2-eq kg^{-1} PET pellets.

Table S19 Input-output of PET flakes to pallet, functional unit = 1 kg TPA*.

Item	Quantity	Unit	Data Source
Input			
PET pallets	1000	kg	Simulation
deionized water	193.7	kg	Simulation and experiment
Electricity, low voltage	730.4	kw·h	Simulation and experiment
Output			
TPA	864.5	kg	Simulation and experiment
FA	108.2	kg	Simulation and experiment
EG	209.8	kg	Simulation and experiment
H_2	11.2	kg	Based on the number of electrons transferred during electrolysis

*Calculation results: Based on the background data from China: NREU 5.70 MJ kg^{-1} TPA; GWP 0.6355 kg CO_2-eq kg^{-1} TPA, Based on the background data from Europe: NREU 2.70 MJ kg^{-1} TPA, GWP 0.2358 kg CO_2-eq kg^{-1} TPA.

Table S20 NREU values of each raw material of PET hydrolysis process used in the OpenLCA.

Process	Value	Unit	Location
chloralkali electrolysis, mercury cell, sodium hydroxide, without water, in 50% solution state	15.31	MJ kg^{-1}	Rest of world*
	8.93		Europe
market group for electricity, low voltage	8.70	MJ $kw^{-1}h^{-1}$	China
	4.13		Europe without Switzerland
the market for heat, district or industrial, natural gas	0.58	MJ MJ^{-1}	Rest of world
	0.81		Europe without Switzerland
transport, freight, lorry >32 metric ton	1.51	MJ $(t\ km)^{-1}$	Rest of world
	1.49		Europe
treatment of waste polyethylene terephthalate, sanitary landfill	0.26	MJ kg^{-1}	Rest of world
sulfuric acid production	1.28	MJ kg^{-1}	Rest of world
	1.06		Europe
water production, deionized	0.0050	MJ kg^{-1}	Rest of world

*The rest of the world represents China.

Table S21 GWP values of each raw material of the PET hydrolysis process used in the OpenLCA.

Process	Value	Unit	Location
chloralkali electrolysis, mercury cell, sodium hydroxide, without water, in 50% solution state	1.47	$kgCO_2$-eq kg^{-1}	China
	0.81		Europe
market group for electricity, low voltage	0.97	$kgCO_2$-eq $kw^{-1}h^{-1}$	China
	0.36		Europe without Switzerland
the market for heat, district or industrial, natural gas	0.038	$kgCO_2$-eq MJ^{-1}	China
	0.055		Europe without Switzerland
transport, freight, lorry >32 metric ton	0.10	$kgCO_2$-eq $(t*km)^{-1}$	China
	0.10		Europe
treatment of waste polyethylene terephthalate, sanitary landfill	0.09	$kgCO_2$-eq kg^{-1}	China
sulfuric acid production	0.11	$kgCO_2$-eq kg^{-1}	China
	0.091		Europe
water production, deionized	0.00047	$kgCO_2$-eq kg^{-1}	China

Table S22 Costs in the PET hydrolysis process.

Raw materials	Quantity	Unit	Unit price	Cost (USD)	Cost (USD $ton^{-1}PET^{-1}$)
PET pallets	5700	Metric ton	-	2850000	500
Electricity	8.26	Million kilowatt-hour	69061	570444	100.08
The heat from natural gas	333.88	kilostere	1160	387301	67.95
NaOH (30%)	17.61	Metric ton	442	7784	1.37
Sulfuric acid (30%)	2.60	Metric ton	35.91	93	0.016
2.34Deionized water	1068.75	Metric ton	0.41	438	0.077
Electrolyzer cost	——	——	——	11115	1.95
The catalyst and membrane costs	——	——	——	555.8	0.0975
Reaction tank costs	——	——	——	1111.5	0.195
Separation equipment cost	——	——	——	1111.5	0.195
Operation cost	——	——	——	382983	67.19
Total costs	——	——	——	4212937	739.1

The system operates for 8000 hours annually.

Electrolyzer: I=800 A, U=156 V, P=125 kW, number of electrode plates=164, area=1 m^2.

The cost of the electrolyzer is assumed to be 677 USD per m^{-2} [24] (It is assumed that the electrolyzer can be run for 10 years).

The catalyst and membrane costs are considered to be 5% of electrolyzer cost.[24]

Separation equipment cost will be set as 10% of electrolyzer cost.[24]

Reaction tank costs will be set as 10% of electrolyzer cost.[24]

Operation cost is assumed to be 10% of the capital costs.[24]

Table S23 Profits from the PET hydrolysis process.

Product	Quantity (per year)	Unit	Unit price (USD)	Revenue (USD)	Revenue (USD $ton^{-1}PET^{-1}$)
TPA	4950	Metric ton	1260	6237000	1094.2
Hydrogen	64	Metric ton	1900	121600	21.33
FA	620	Metric ton	399	247380	43.4
EG	1200	Metric ton	640	768000	134.74
Total	——	——	——	7373980	1293.67
Profit per ton PET	——	——	——	——	554.57

References

1. M. S. Islam, Z. Islam, R. Hasan, A. H. M. S. Islam Molla Jamal, *Prog. Rubber Plast. Re.*, 2022, **39**, 12-25.
2. A. Kumar, T. R. Rao, *J. Appl. Polym.*, 2003, **87**, 1781-1783.
3. W. S. Yang, J. Wang, L. Jiao, Y. Song, C. Li, C. Q. Hu, *Green Chem.*, 2022, **24**, 1362-1372.
4. W. S. Yang, R. Liu, C. Li, Y. Song, C. Q. Hu, *Waste Manage.*, 2021,**135**, 267-274.
5. M. Rollo, F. Raffi, E. Rossi, M. Tiecco, E. Martinelli, G. Ciancaleoni, *Chem. Eng. J.*, 2023, **456**, 141092.
6. Y. Peng, J. Yang, C. Deng, J. Deng, L. Shen, Y. Fu, *Nat. Commun.*, 2023, **14**, 3249.
7. H. Abedsoltan, I. S. Omodolor, A. C. Alba-Rubio, M. R. Coleman, *Polymer*, 2021, **222**, 123620.
8. T. Yoshioka, T. Motoki, A. Okuwaki, *Ind. Eng. Chem. Res.*, 2001, **40**, 75-79.
9. T. Yoshioka, N. Okayama, A. Okuwaki, *Ind. Eng. Chem. Res.*, 1998, **37**, 336-340.
10. Y.-J. Luo, J.-Y. Sun, Z. Li, *Green Chem. Eng.*, 2023, **5**, 257-265.
11. S. Mishra, A. S. Goje, V. S. Zope, *Polym-Plast. Technol.*, 2003, **42**, 581-603.
12. A. Barredo, A. Asueta, I. Amundarain, J. Leivar, R. Miguel-Fernández, S. Arnaiz, E. Epelde, R. López-Fonseca, J. I. Gutiérrez-Ortiz, *J. Environ.*, 2023, **11**, 109823.
13. Y. Wang, H. Wang, H. Chen, H. Liu, *Chin. J. Chem. Eng.*, 2022, **51**, 53-60.
14. S. Ügdüler, K. M. Van Geem, R. Denolf, M. Roosen, N. Mys, K. Ragaert, S. De Meester, *Green Chem.*, 2020, **22**, 5376-5394.
15. L. Cosimbescu, D. R. Merkel, J. Darsell, G. Petrossian, *Ind. Eng. Chem.*, 2021, **60**, 12792-12797.
16. H. Zhou, Y. Ren, Z. Li, M. Xu, Y. Wang, R. Ge, X. Kong, L. Zheng, H. Duan, *Nat. Commun.*, 2021, **12**, 4679.
17. Y. Du, Q. Chen, L. Shen, Y. Xing, J. Dai, *J. Appl. Polym.*, 2011, **121**, 2927-2935.
18. I. Corak, A. Tarbuk, D. Dordevic, K. Visic, L. Botteri, *Materials (Basel)*, 2022, **15**, 1503 .
19. R. López-Fonseca, M. P. González-Marcos, J. R. González-Velasco, J. I. Gutiérrez-Ortiz, *J. Chem. Technol.*, 2008, **84**, 92-99.
20. G. P. Karayannidis, A. P. Chatziavgoustis, D. S. Achilias, *Adv. Polym. Tech.*, 2002, **21**, 250-259.
21. N. R. Paliwal, A. K. Mungray, *Polym. Degrad. Stabil.*, 2013, **98**, 2094-2101.
22. X. Liu, X. He, D. Xiong, G. Wang, Z. Tu, D. Wu, J. Wang, J. Gu and Z. Chen, *ACS Catal.*, 2024, **14**, 5366-5376.
23. K. Liu, Y. Wang, F. Liu, C. Liu, R. Shi and Y. Chen, *Chem. Eng. J.*, 2023, **473**, 145292.
24. S. L. Kang, X. Y. Guo, D. Xing, W. F. Yuan, J. Shang, V. Nicolosi, N. Zhang and B. C. Qiu, *Small*, **2024**, 20, 2406068.

25. X. Lu, Y. Guo, H. Fu, J. Song, C. Liang, H. Jiang, Z. Wang, Y. Liu, H. Cheng, Z. Zheng, Y. Wu, P. Wang and B. Huang, *Chem. Eng. J.*, 2025, **506**, 159810.

26. J. Wang, X. Li, T. Zhang, Y. Chen, T. Wang and Y. Zhao, *J. Phys. Chem. Lett.*, 2022, **13**, 622-627.

27. H. Zhang, Y. Wang, X. Li, K. Deng, H. Yu, Y. Xu, H. Wang, Z. Wang and L. Wang, *Appl. Catal. B Environ.*, 2024, **340**, 123236.

28. J. Fan, B. Xu, C. Cheng and Y. Wang, *Appl. Catal. B E-Energy*, 2025, **367**, 125076.

29. J. Chang, L. Wang, D. Wu, F. Xu, K. Jiang, Y. Guo and Z. Gao, *J. Colloid Interface Sci.*, 2024, **655**, 555-564.

30. X. Hu, L. L. Liao, L. M. Yang, B. Y. Xia and B. You, *Green Chem.*, 2025,**27**, 2493-2503.

31. S. Behera, S. Dinda, R. Saha and B. Mondal, *ACS Catal.*, 2023, **13**, 469-474.

32. D. Bajuk-Bogdanovic, S. Uskokovic-Markovic, R. Hercigonja, A. Popa and I. Holclajtner-Antunovic, *Spectrochimica Acta. A*, 2016, **153**, 152-159.

33. L. Shen, E. Nieuwlaar, E. Worrell, M. K. Patel, *Int. J. Life Cycle Assess.*, 2011, **16**, 522-536.